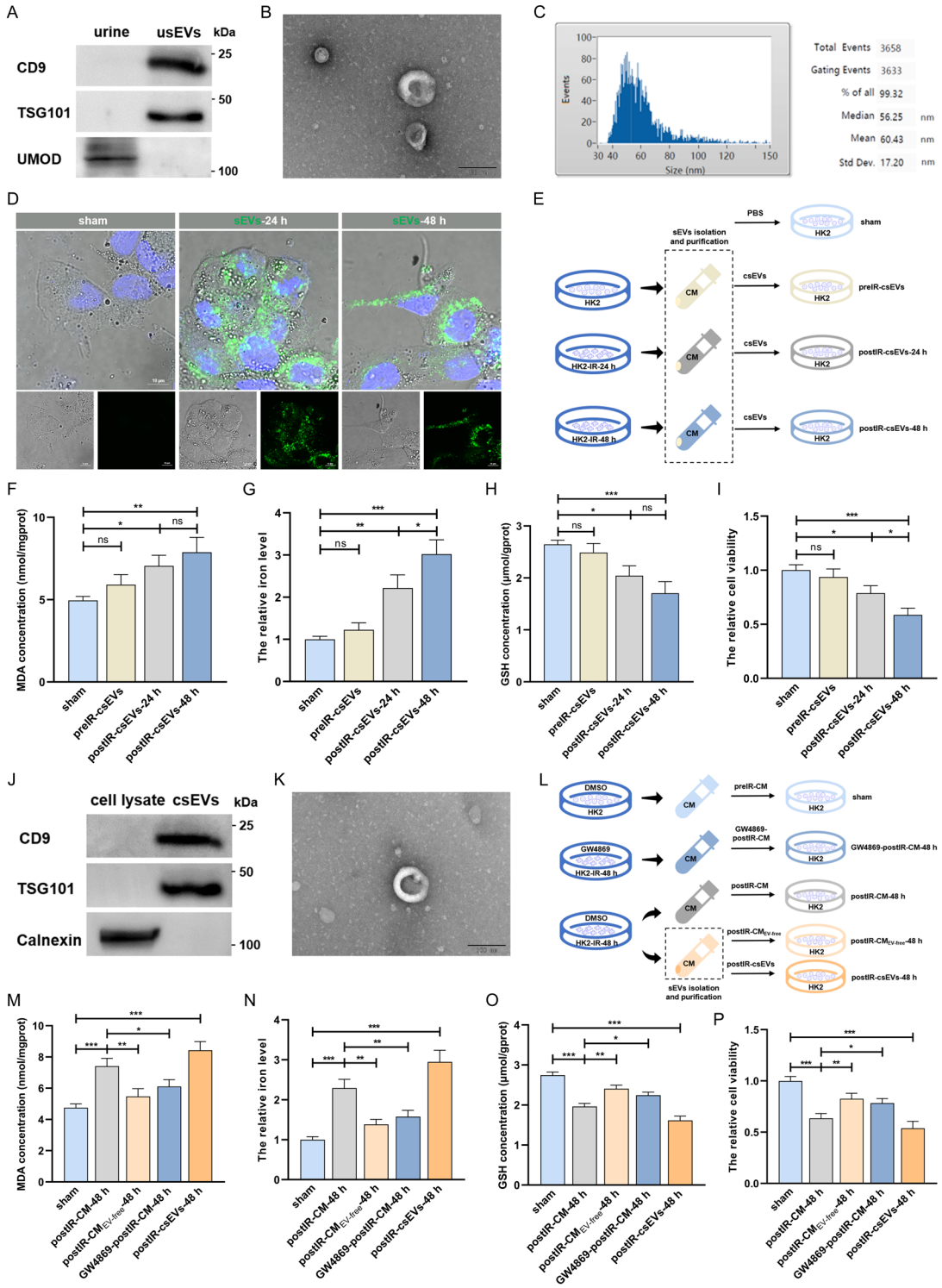

Figure S1. IRI-sEVs induce ferroptosis in normal renal tubular epithelial cells. (A) IB illustrating the expression of three categories of usEV markers (CD9, TSG101, and UMOD). (B) usEV morphologies were observed by TEM; scale bar: 100 nm. (C) Flow NanoAnalyzer showing the

particle size ranges of usEVs. (D) IF assays recording the intracellular uptake of sEVs (labeled with PKH67, green) by HK-2 cells; scale bar: 10 μm. (E) Schematic showing the flow to construct the in vitro intervention model using HK-2 cells and csEVs derived from different HK-2 cell supernatant; preIR-csEVs: csEVs isolated from HK-2 cells without ischemia-reperfusion treatment, postIR-csEVs-24/48 h: csEVs isolated from HK-2 cells 24/48 h after ischemia-reperfusion administration. (F-I) MDA concentration, iron level, GSH concentration and cell viability were detected in HK-2 cells following csEV treatments ($n = 6$ group^{-1}); the result of iron level and cell viability was normalized according to the result of sham; one-way ANOVA followed by Tukey's test. The csEV marker proteins and morphologies were examined by IB assays (J) and TEM (K) respectively. (L) Different CM and csEVs were employed to treat HK-2 cells and simulated the renal tissue microenvironment in vitro. (M-P) MDA concentration, iron level, GSH concentration and cell viability were detected in HK-2 cells after distinct treatments ($n = 6$ group^{-1}); the result of iron level and cell viability was normalized according to the result of sham; one-way ANOVA followed by Tukey's test. ***$p < 0.001$, **$p < 0.01$, and *$p < 0.05$ represent significant differences between two groups; ns represents no significant difference.

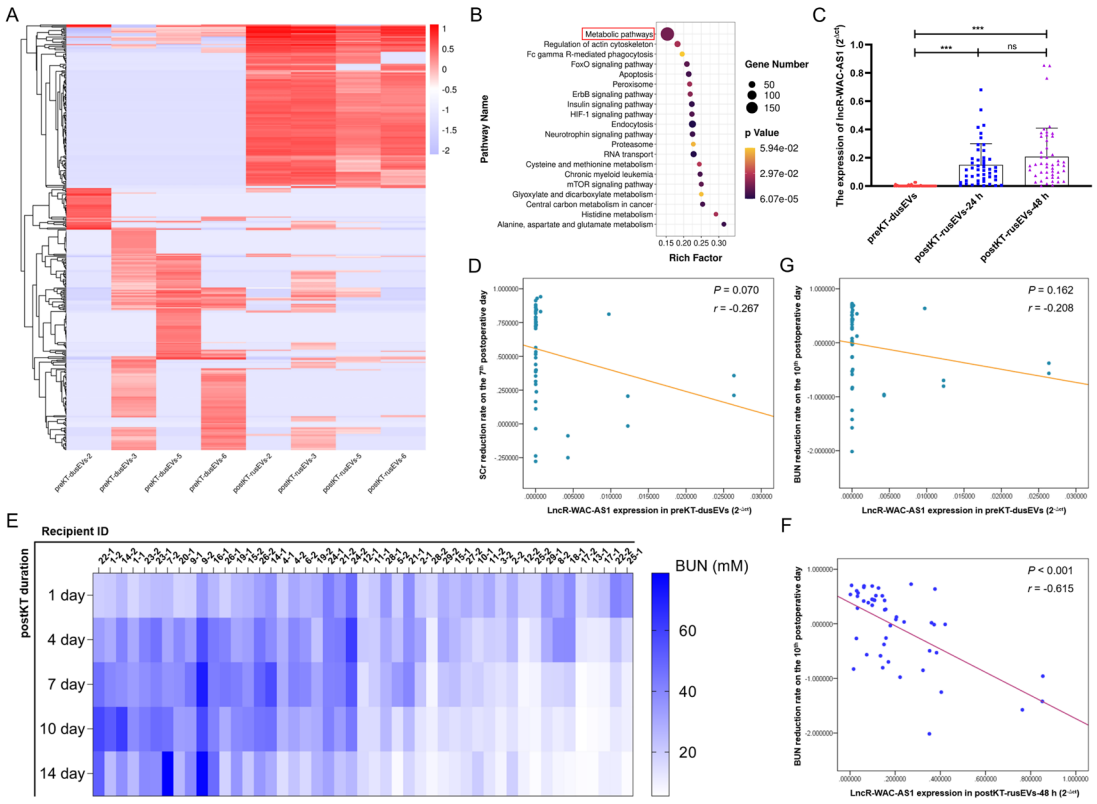

Figure S2. LncRNA-WAC-AS1 enriched in IRI-sEVs impedes graft function recovery. (A) Cluster heatmap delineating all identified differential lncRNAs between the paired preKT-dusEVs (n = 4) and postKT-rusEVs (n = 4). (B) Kyoto Encyclopedia of Genes and Genomes (KEGG) analysis of upregulated lncRNAs in postKT-rusEVs. (C) Quantitative analysis of the level of lncRNA-WAC-AS1 in the paired preKT-dusEVs (n = 29), postKT-rusEVs-24 h (n = 47) and postKT-rusEVs-48 h (n = 47) by unpaired 2-tailed Student's t test. (D) Correlation analysis between lncR-WAC-AS1 level in preKT-dusEVs and the SCr recovery rate on the 7th postoperative day (n = 47). (E) Heatmap illustrating the BUN concentration of recipients after kidney transplantation. Correlation analysis between the BUN reduction rate on the 10th postoperative day (n

= 47) and the lncR-WAC-AS1 level in preKT-dusEVs (F) and postKT-rusEVs-48 h (G). ***$p < 0.001$ represents significant differences between two groups; ns represents no significant difference.

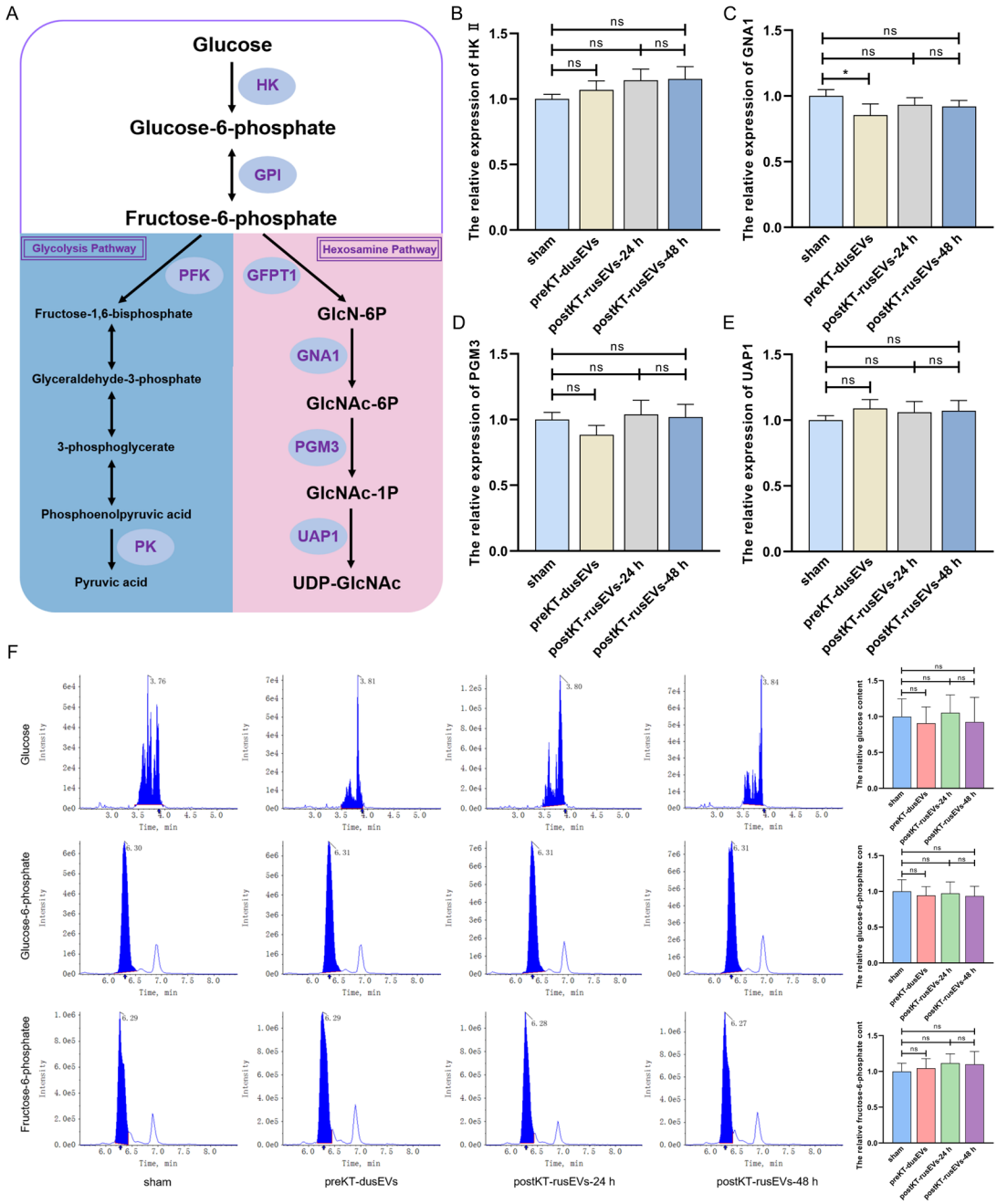

Figure S3. IRI-sEVs have no effects on other metabolic enzymes before and in the HBP branch. (A) Schematic representation of HBP and

glycolysis pathway in the glucose metabolism process. (B-E) The transcriptional levels of some glucose metabolic enzymes in HK-2 cells before and after 47 pairs of usEV treatments; the results were normalized according to the result of sham; one-way ANOVA followed by Tukey's test. (F) The contents of glucose metabolic metabolites before the HBP branch (left) and quantitative analysis (right); one-way ANOVA followed by Tukey's test. *$p < 0.05$ represents significant differences between two groups; ns represents no significant difference.

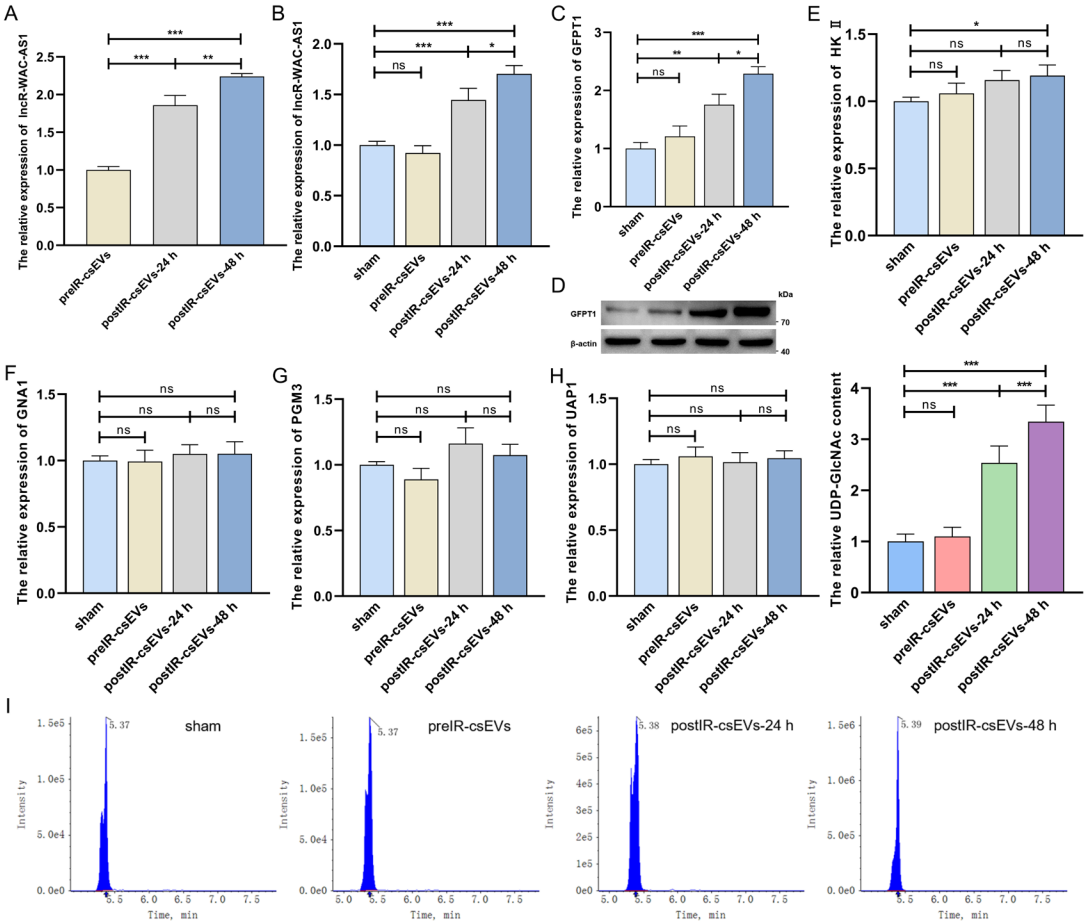

Figure S4. IRI-sEVs accelerate HBP metabolism by upregulating GFPT1 in normal renal tubular epithelial cells. (A) The relative level of

lncR-WAC-AS1 in preIR-csEVs, postIR-csEVs-24 h and postIR-csEVs-48 h (n = 6 group^{-1}); the results were normalized according to the lncR-WAC-AS1 level in preIR-csEVs; one-way ANOVA followed by Tukey's test. The relative lncR-WAC-AS1 level (B), GFPT1 expression (C-D) and the transcriptional levels of other glucose metabolic enzymes (E-H) in HK-2 cells following different csEV treatments (n = 6 group^{-1}); the results were normalized according to the result of sham; one-way ANOVA followed by Tukey's test. (I) The UDP-GlcNAc content in HK-2 cells after csEV treatments (bottom) and quantitative analysis (top); the UDP-GlcNAc level was normalized according to the sham; one-way ANOVA followed by Tukey's test. ***$p < 0.001$, **$p < 0.01$, and *$p < 0.05$ represent significant differences between two groups; ns represents no significant difference.

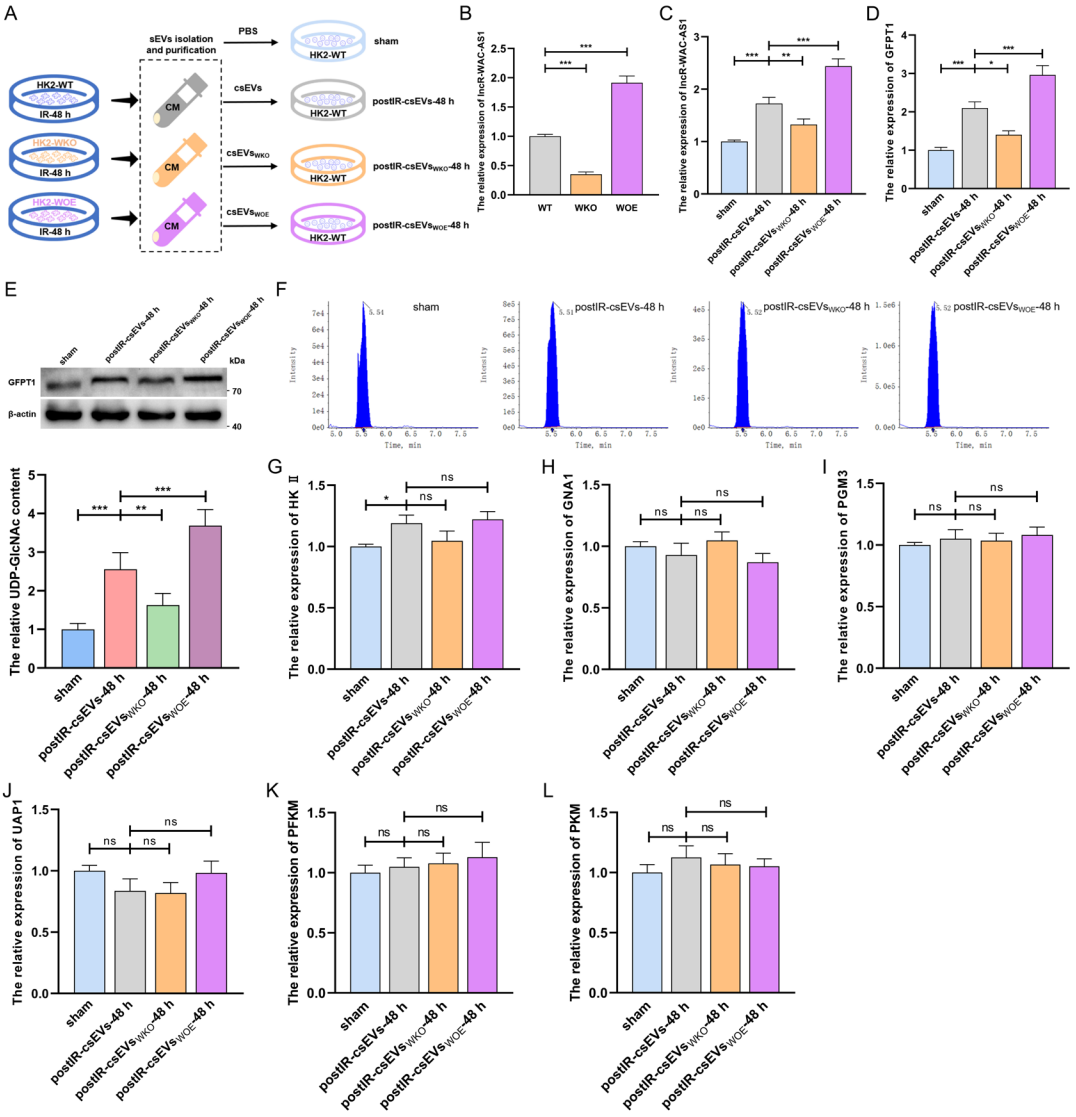

Figure S5. LncRNA-WAC-AS1 enriched in IRI-sEVs induce GFPT1 and thus facilitate HBP metabolic reprogramming in normal renal tubular epithelial cells. (A) Schematic delineating the flow to establish the in vitro intervention model using HK-2 cells and csEVs derived from different HK-2 cells; csEVs$_{WKO}$: csEVs isolated from lncRNA-WAC-AS1- knockout HK-2 cells, csEVs$_{WOE}$: csEVs isolated from HK-2 cells with stable overexpression of lncRNA-WAC-AS1 (WOE). (B) The relative level of lncRNA-WAC-AS1 in different HK-2 cells (n = 6 group-

[1]); the results were normalized according to the lncR-WAC-AS1 level in WT; one-way ANOVA followed by Tukey's test. The relative lncR-WAC-AS1 level (C), GFPT1 expression (D-E), UDP-GlcNAc content (F) and the transcriptional levels of other glucose metabolic enzymes (G-L) in HK-2 cells after distinct csEV treatments (n = 6 group^{-1}); the results were normalized according to the result of sham; one-way ANOVA followed by Tukey's test. ***$p < 0.001$, **$p < 0.01$, and *$p < 0.05$ represent significant differences between two groups; ns represents no significant difference.

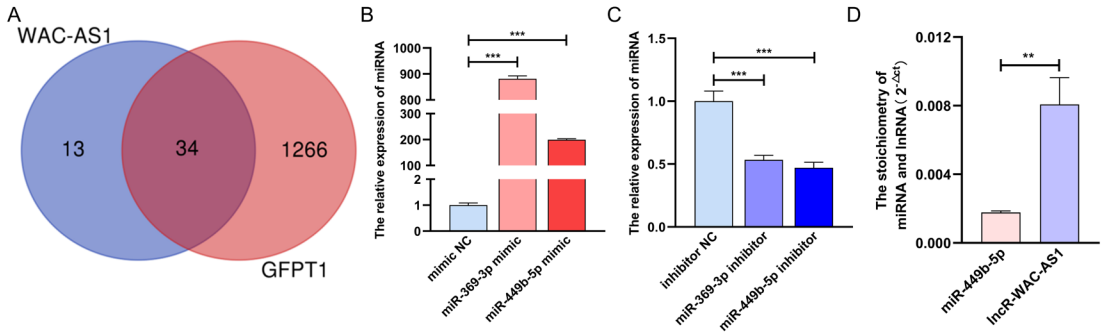

Figure S6. LncRNA-WAC-AS1 modulates GFPT1 by competitively binding to miRNAs. (A) Venn diagram illustrating the predicted miRNAs bound to lncRNA-WAC-AS1 and GFPT1 in the Starbase database. (B-C) The relative levels of miRNAs in HK-2 cells transfected with miRNA mimics and inhibitors (n = 6 group^{-1}); the expression levels were normalized according to the result in mimic NC or inhibitor NC; one-way ANOVA followed by Tukey's test. (D) The expression levels of miR-449b-5p and lncRNA-WAC-AS1 in HK-2 cells (n = 6 group^{-1}); unpaired 2-tailed

Student's t test. ***$p < 0.001$ and **$p < 0.01$ represent a significant difference between two groups.

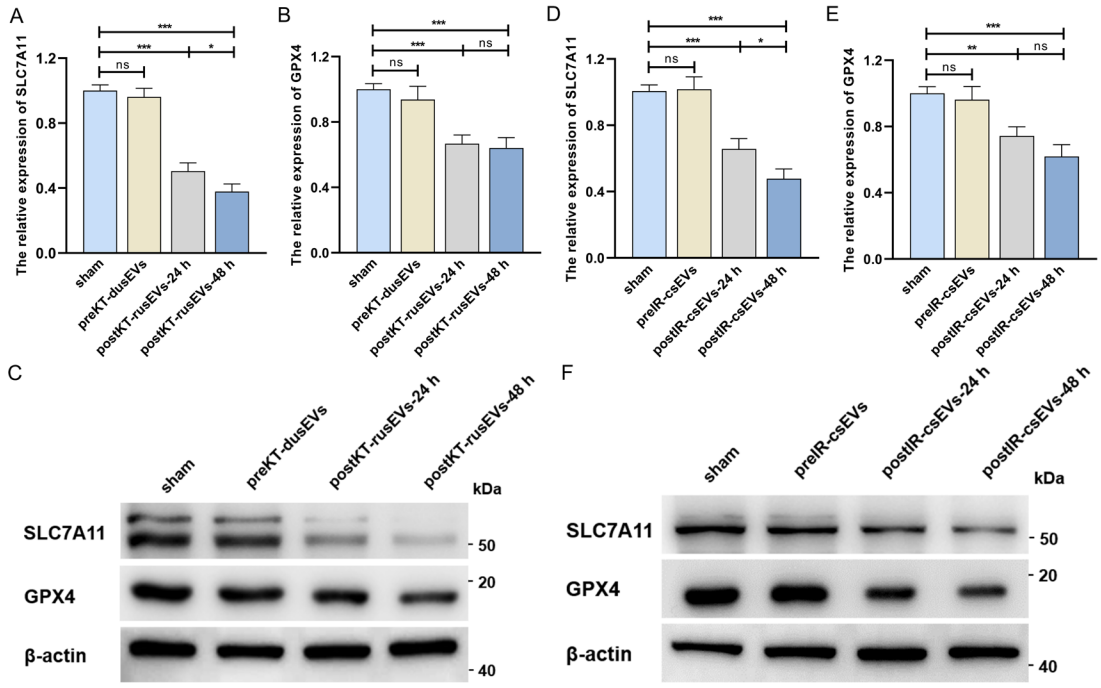

Figure S7. IRI-sEVs inhibit the expression of SLC7A11 and GPX4 in normal renal tubular epithelial cells. The transcriptional (A-B) and translational (C) levels of SLC7A11 and GPX4 in HK-2 cells following 47 pairs of usEV treatments; one-way ANOVA followed by Tukey's test. The mRNA levels of SLC7A11 (D) and GPX4 (E) in HK-2 cells after csEV administrations were normalized according to the level of sham (n = 6 group^{-1}); one-way ANOVA followed by Tukey's test. (F) IB assays detecting the protein expression of SLC7A11 and GPX4. ***$p < 0.001$, **$p < 0.01$, and *$p < 0.05$ represent significant differences between two groups; ns represents no significant difference.

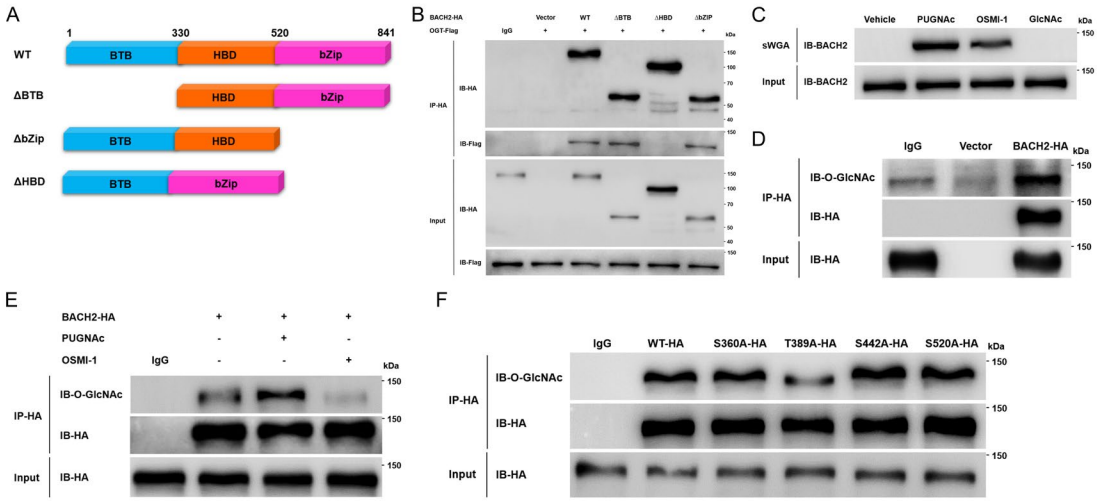

Figure S8. Thr 389 is the key O-GlcNAcylated site on BACH2. (A) Schematic delineating the BACH2 construct. WT BACH2 contains three main domains, including a domain of broad-complex, tramtrack and bric a brac (BTB), a heme-binding domain (HBD) and a basic-leucine zipper domain (bZIP); truncation mutants of BACH2, comprising amino acids 331–841 (ΔBTB), 1–520 (ΔbZIP), and the full-length removal of 331–520 (ΔHBD). (B) Co-IP assays of interactions between OGT and different BACH2 fragments, such as WT BACH2, the ΔBTB, the ΔHBD and the ΔbZIP, in 293T cells. (C) sWGA pull-down assays were conducted in HK-2 cells following treatments with 50 μM PUGNAc or 50 μM OSMI-1 for 24 h. IB assays were performed by anti-BACH2. (D) BACH2 IP assays using anti-HA antibody in 293T cells transfected with BACH2-HA or a vector control. IB assays were determined utilizing anti-O-GlcNAc and anti-HA antibodies. (E) Cell lysates of HK-2 cells administrated with 50 μM PUGNAc or 50 μM

OSMI-1 were immunoprecipitated using an anti-HA antibody followed by IB assays. (F) IP assays using an anti-HA antibody in HK-2 cells transfected with vectors containing BACH2 full-length cDNA fragments or different site-directed mutants.

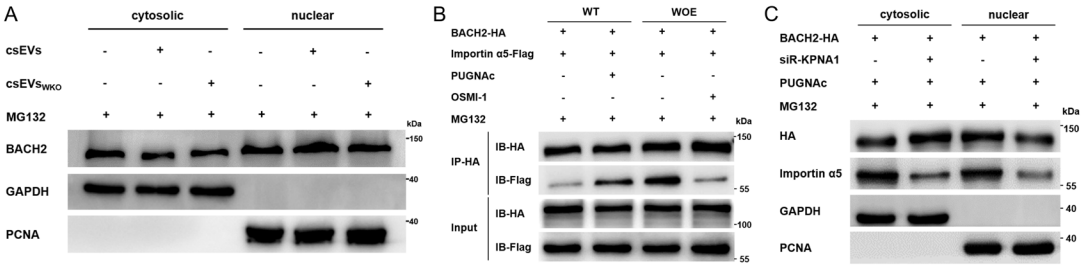

Figure S9. Importin α5 mediates the nuclear translocation of BACH2. (A) IB results illustrating the cytosolic and nuclear levels of endogenous BACH2 in HK-2 cells treated with 40 μM MG132 and 100 μg csEVs either or 100 μg csEVs$_{WKO}$. (B) IP assays using an anti-HA antibody in WT and WOE HK-2 cells co-transfected with BACH2-HA and importin *α*5-Flag after administrations of 40 μM MG132 and 50 μM PUGNAc either or 50 μM OSMI-1. (C) IB assays detected the cytosolic and nuclear levels of HA-tagged BACH2 in HK-2 cells treated with siRNA-KPNA1 or not.

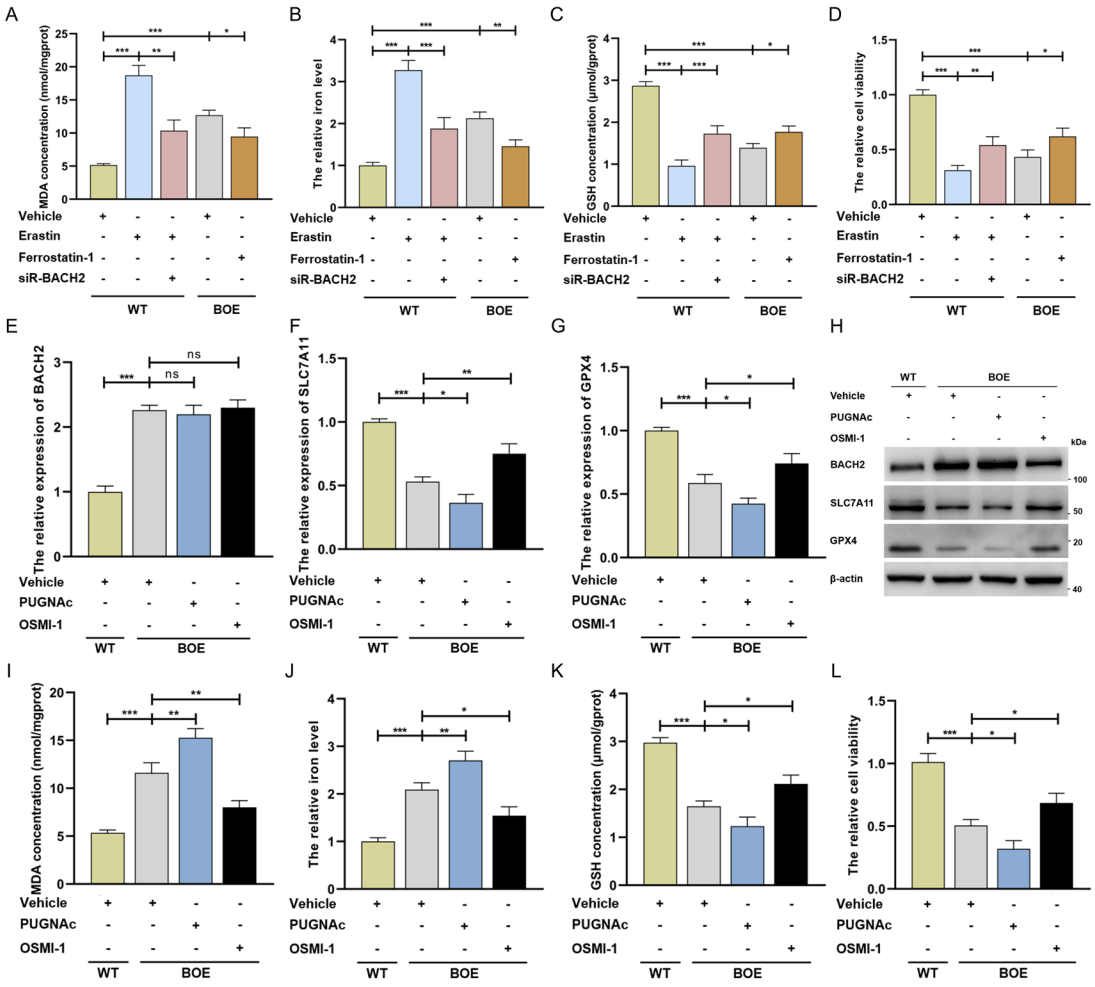

Figure S10. BACH2 O-GlcNAcylation promotes ferroptosis by suppressing transcription of SLC7A11 and GPX4. (A-D) MDA concentration, iron level, GSH concentration and cell viability were determined in HK-2 cells with different expression levels of BACH2 following treatments with 10 μM erastin or 1 μM ferrostatin-1 (n = 6 group^{-1}); the iron level and cell viability were normalized according to the result of WT-vehicle group; one-way ANOVA followed by Tukey's test. The mRNA (E-G) and protein (H) levels of BACH2, SLC7A11 and GPX4, and ferroptosis levels (I-L) in WT and BACH2-overexpressing

HK-2 cells (BOE) after administration of 50 μM PUGNAc or 50 μM OSMI-1 (n = 6 group^{-1}); one-way ANOVA followed by Tukey's test. ***$p < 0.001$, **$p < 0.01$, and *$p < 0.05$ represent significant differences between two groups; ns represents no significant difference.

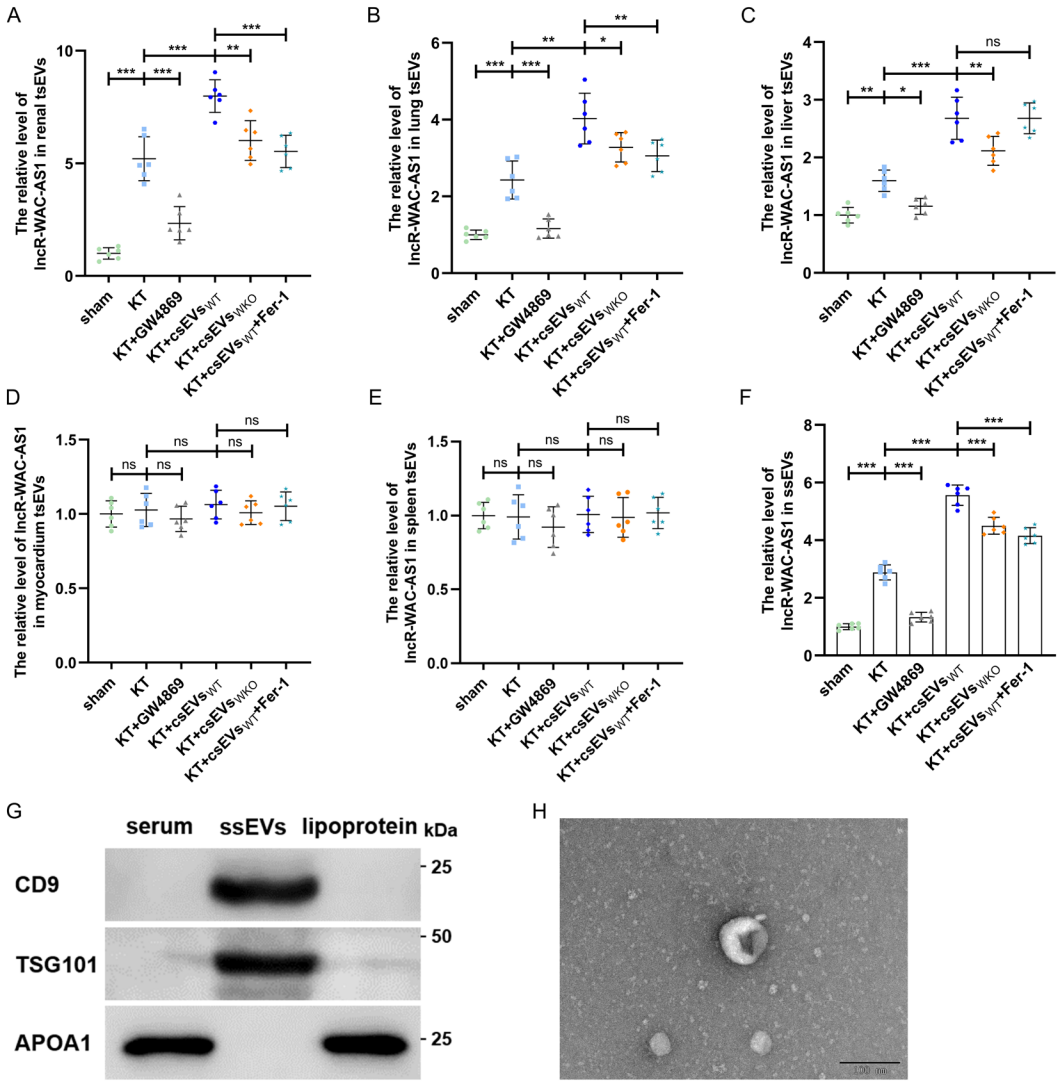

Figure S11. IRI-sEVs lead to the systemic spread of lncRNA-WAC-AS1 during mouse kidney transplantation. The relative levels of lncR-WAC-AS1 in tsEVs derived from graft renal (A), lung (B), liver (C), myocardium (D) and spleen (E), and serum-derived sEVs (ssEVs, F) were

normalized according to the levels of sham (n = 6 group^{-1}); one-way ANOVA followed by Tukey's test. The ssEV marker proteins and morphologies were detected by IB assays (G) and TEM (H) respectively. ***$p < 0.001$, **$p < 0.01$, and *$p < 0.05$ represent significant differences between two groups; ns represents no significant difference.

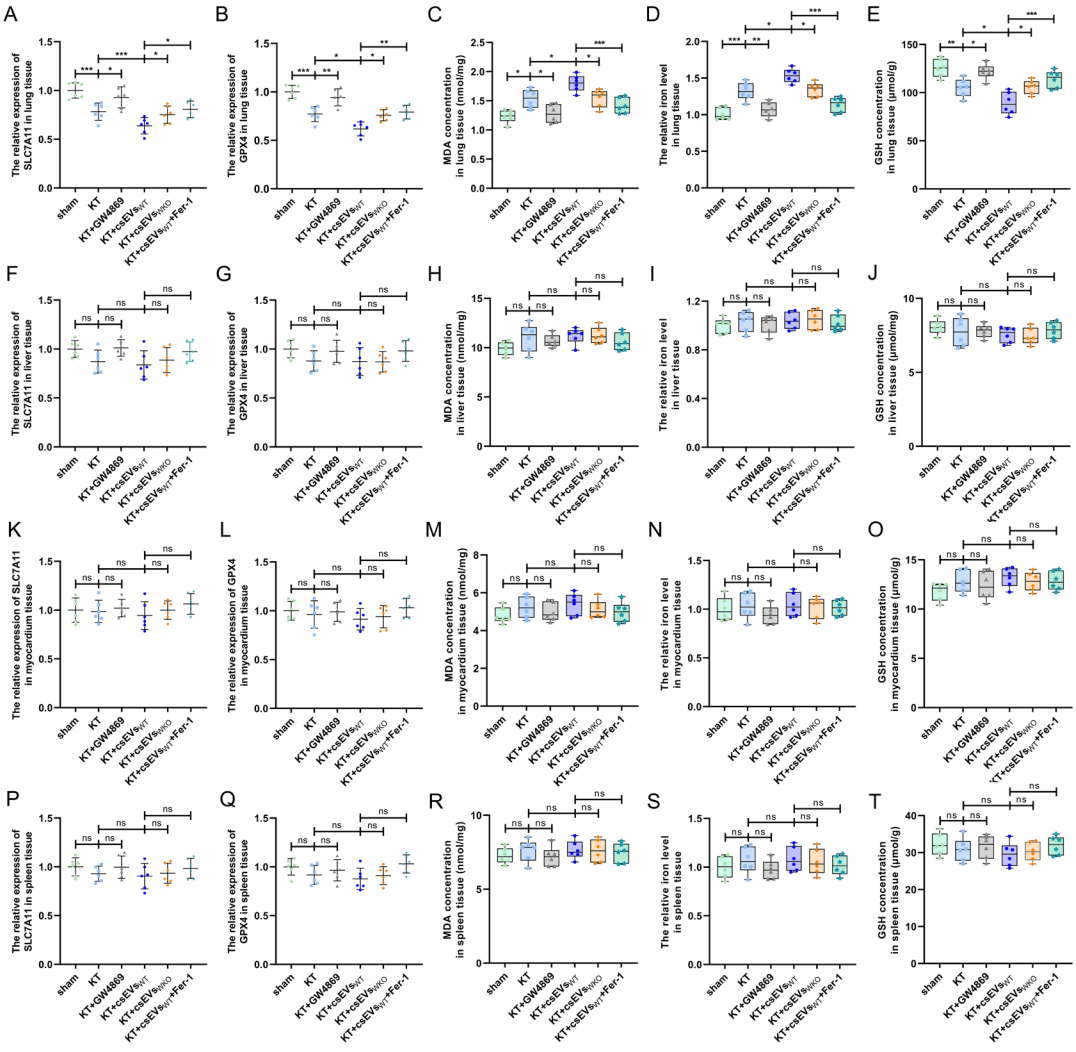

Figure S12. IRI-sEVs promote "wave of ferroptosis" propagation from kidney to lung. The SLC7A11 and GPX4 expression, MDA concentration, iron level and GSH concentration in lung tissues (A-E), liver tissues (F-J),

myocardium tissues (K-O) and spleen tissues (P-T) of recipient mice were normalized according to the levels of sham (n = 6 group^{-1}); one-way ANOVA followed by Tukey's test. ***$p < 0.001$, **$p < 0.01$, and *$p < 0.05$ represent significant differences between two groups; ns represents no significant difference.

Table S1: The sequence of sgRNA, siRNA and primer

Item		Sequence
sgRNA		
WAC-AS1-sgRNA-1		CACCGAATGTAGAAAACGCT
WAC-SA1-sgRNA-2		CGTGCACGCATCTCCGCTGA
GAL4-sgRNA		AACGACTAGTTAGGCGTGTA
siRNA		
siR-KPNA1-1		GCAUGUUGGACGAUAUCUAAU
siR-KPNA1-2		GGUUUGUGGAGUUCCUCAAAC
siR-BACH2-1		GGCGCUGGUUGGACAGACAAA
siR-BACH2-2		GGGAAGAUAACUCUAGCAACA
Primer		
lncR-WAC-AS1	Forward	CCATTTCTTCCCCTGGGCTT
	Reverse	TTAAGGTGCCTGCCTGTCTG
miR-369-3p	Forward	TTGAAGGGAGATCGACCGTGT
	Reverse	CTGAGAAAAGATCAACCATGT
miR-449b-5p	Forward	CTGTGTGTGATGAGCTGGCAG
	Reverse	TGTATATGCAATAAGACAGCA
GFPT1	Forward	TCCCTTGTGATGTTTGCCCT
	Reverse	TCAGTGCCCCTTCAAGACAA
BACH2	Forward	CTTTCTTTCAGGGTGTGAACGGC
	Reverse	CAGAGCCGAGTCACTAGGTATAA
SLC7A11-1	Forward	ATGCAGTGGCAGTGACCTTT
	Reverse	GGCAACAAAGATCGGAACTG
SLC7A11-2	Forward	TTGTTTTGCACCCTTTGACA
	Reverse	AAAGCTGGGATGAACAGTGG
GPX4-1	Forward	CGGAATTCATGAGCCTCGGCCGCCTTTG

	Reverse	CCGCTCGAGGAAATAGTGGGGCAGGTCCT
GPX4-2	Forward	GTAACCAGTTCGGGAAGCAG
	Reverse	TGTCGATGAGGAACTGTGGA
HK Ⅱ	Forward	GCCCGCCAGAAGACATTAG
	Reverse	TGCTCAGACCTCGCTCCAT
GAN1	Forward	CATCCTGGAGAAGGCTTGGTT
	Reverse	GCTGACAACTCCAGTCTCTGT
PGM3	Forward	GGCCGATATGGAAAGGCAAC
	Reverse	GCCATTTGCACAGTCAACCT
UAP1	Forward	ACCAGTGGCAGAACAATGGA
	Reverse	AGTGCCCGATAAAGACCACC
PFKM	Forward	GGTGGATGGTGGAGATCACA
	Reverse	TTCCCGAAAGTCCTTGCACC
PKM	Forward	ACGTGGATGATGGGCTTATTTCT
	Reverse	ACGCAAACACCATATCAACATCC
β-actin-1	Forward	CCTTCCTGGGCATGGAGTC
	Reverse	TGATCTTCATTGTGCTGGGTG
β-actin-2	Forward	CCACCATGTACCCAGGCATT
	Reverse	CAGCTCAGTAACAGTCCGCC

Table S2 Gene sequence used in luciferase reporter assay

Gene	Sequence (5'-3')
SLC7A11-WT	TAAATGATGAAGACCTAACCGATTTTAGAGAAATTTCACACACG AAACAAGAGATTTTTCGAATCCAGTCAACTCGTTGTTCGAGGAG GACAAAAAAAAGAAAAAAATTTTTTTTCTCGACTCATTACGACCTC CGAAGAGTACACCGACTACGTTTGGACCTCTTAAACGTAGTAGTA AATCGACATCATTCAACCACAC
SLC7A11-MT	TAAATGATGAAGACCTAACCGATTTTAGAGAAATTTCACACACG AAACAAGAGATTTTTCGAATCCAGTCAACTCGTTGTTCGAGGAG GACAAAAAAAAGAAAAAAATTTTTTTTAGAGCTGAGTAATGGACCTC CGAAGAGTACACCGACTACGTTTGGACCTCTTAAACGTAGTAGTA AATCGACATCATTCAACCACAC
GPX4-WT	GAGCTGCGATGGAGCCACTGCACTCCAGCCTGGGTGACAGAC CAAGACTCCTCAAAAAAAAAAAAAAAAATCCAAACCCCTGCCT GTACAGGGGTCAAAGTCCAATCACGGTGACTCAGTTCCCAAGT ATGAGATGAGTGTTTCTGTTGCCACATGTCCAAGCCACGAAGTG AAAAACAGAGTTGGAAGCCAAGATGTGG
GPX4-MT	GAGCTGCGATGGAGCCACTGCACTCCAGCCTGGGTGACAGACC AAGACTCCTCAAAAAAAAAAAAAAAAATCCAAACCCCTGCCTGT ACAGGGGTCAAAGTCCAATCACAACAGTCTGACCTTCAAGTAT GAGATGAGTGTTTCTGTTGCCACATGTCCAAGCCACGAAGTGA AAAACAGAGTTGGAAGCCAAGATGTGG
lncR-WAC-AS1-WT	GCGGGGAGCGCCGCUCGGGGCAGGGAAUGAAAGCGGCGCUUG AGACUGGAAAUUUAGGGAGAUGAGUUCCUUGGGAACAACGCUG AACCAUCUCACUGCCCCACCCUACCCCUUGUUAUUUUUUUUUGA GACAGGUCUCGCGCUGUCGUCCAGUCUGAGUGCAGUGACGCGA UCACGGCUCACUGCAGCCUCGACCUCCG
lncR-WAC-AS1-MT	GCGGGGAGCGCCGCUCGGGGCAGGGAAUGAAAGCGGCGCUUG AGACUGGAAAUUUAGGGAGAUGAGUUCCUUGGGAACAACCGAG UUGCUACUGUGACGGCCACCCUACCCCUUGUUAUUUUUUUUUGA GACAGGUCUCGCGCUGUCGUCCAGUCUGAGUGCAGUGACGCGA UCACGGCUCACUGCAGCCUCGACCUCCG
GFPT1-WT	GUUAUGUUAGAAAUUGUAUUGUACUAAGAAUGUAAUCAAUGUCU ACUUUAGUUGUAAACAUUUCUGAUGUCAAAACUUUAUUCAUUAC UGUUGAUUUUAAGAAUAAGAAAUCACUGCCUAAAUAUUACCAAA AGCCACUGUCUCUACCCGAACUUCCCAGUUUGGGAAAGAAUCGU UAGAUAAAACAAAGGCUCUGCCCU
GFPT1-MT	GUUAUGUUAGAAAUUGUAUUGUACUAAGAAUGUAAUCAAUGUCU ACUUUAGUUGUAAACAUUUCUGAUGUCAAAACUUUAUUCAUUAC UGUUGAUUUUAAGAAAUUGUUAUGUGACGGUAAAUAUUACCAAA AGCCACUGUCUCUACCCGAACUUCCCAGUUUGGGAAAGAAUCGU UAGAUAAAACAAAGGCUCUGCCCU
BACH2	ATGTCTGTGGATGAGAAGCCTGACTCCCCCATGTATGTGTATGAGT CCACAGTCCACTGCACCAACATCCTCCTGGGCCTCAATGACCAGC

GGAAAAAGGATATTCTCTGTGACGTGACTTTGATCGTGGAGAGG
AAGGAGTTCCGGGCCCACCGGGCTGTGCTGGCCGCATGCAGTG
AATATTTTTGGCAGGCGCTGGTTGGACAGACAAAAAATGATTTG
GTGGTCAGCTTGCCTGAGGAGGTCACAGCCAGGGGCTTTGGGC
CGCTGTTACAGTTTGCCTACACTGCCAAGCTGTTACTCAGCAGA
GAAAACATCCGCGAGGTCATCCGCTGTGCTGAGTTCCTGCGCAT
GCACAACCTGGAGGACTCCTGCTTCAGCTTCCTGCAGACCCAGC
TCCTGAACAGTGAGGATGGCCTGTTTGTGTGCCGGAAGGATGC
TGCGTGCCAGCGCCCACACGAGGACTGCGAGAACTCTGCAGGAG
AGGAGGAGGATGAAGAGGAGGAGACGATGGATTCAGAGACGGCC
AAGATGGCTTGCCCCAGGGACCAGATGCTTCCAGAGCCCATCAGC
TTTGAGGCCGCCGCCATCCCCGTAGCAGAGAAGGAAGAAGCCCTG
CTGCCCGAGCCTGACGTGCCCACAGACACCAAGGAGAGCTCAGAA
AAGGACGCGTTAACGCAGTACCCCAGATACAAGAAATACCAGCTTG
CATGTACCAAGAATGTCTATAATGCATCATCACACAGTACCTCAGGT
TTTGCAAGCACATTCCGGGAAGATAACTCTAGCAACAGCCTCAAG
CCGGGGCTTGCCAGGGGGCAGATTAAAAGTGAGCCGCCCAGTGA
AGAGAATGAGGAAGAGAGCATCACGCTCTGCCTGTCTGGAGATGA
GCCTGACGCCAAGGACAGAGCGGGGGATGTCGAGATGGACCGGA
AACAGCCCAGCCCTGCCCCTACCCCCACGGCCCCAGCTGGGGCCG
CCTGCCTGGAGAGATCCAGGAGCGTGGCCTCGCCCTCCTGCTTAA
GGTCTCTGTTCAGCATAACGAAAAGTGTGGAGCTGTCTGGCCTGC
CCAGTACATCTCAGCAGCACTTTGCCAGGAGTCCAGCCTGCCCTT
TTGACAAGGGGATCACTCAGGGTGACCTTAAAACTGACTACACCC
CTTTCACAGGGAATTATGGACAGCCCCACGTGGGCCAGAAGGAGG
TGTCCAACTTCACCATGGGGTCGCCCCTCAGGGGGCCTGGGTTG
GAGGCTCTCTGTAAACAGGAGGGAGAGCTGGACCGGAGGAGCGT
GATCTTCTCCTCCAGCGCTTGTGACCAAGTGAGCACCTCGGTGCA
TTCTTATTCTGGGGTGAGCAGTTTGGACAAAGACCTCTCTGAGCC
GGTGCCAAAGGGTCTGTGGGTGGGAGCCGGCCAGTCCCTCCCCA
GCTCGCAGGCCTACTCCCACGGTGGGCTGATGGCCGACCACTTGC
CAGGAAGGATGCGGCCCAACACCAGCTGCCCGGTACCAATCAAAG
TCTGCCCTCGCTCACCCCCCTTGGAGACCAGGACCAGGACTTCCA
GCTCCTGCTCTTCCTATTCCTACGCGGAGGACGGGAGCGGGGGCT
CACCCTGCAGCCTCCCTCTCTGTGAGTTCTCCTCCTCGCCCTGTTC
CCAGGGAGCCAGATTCCTTGCCACAGAACATCAGGAACCAGGCCT
GATGGGAGATGGAATGTACAACCAAGTGCGGCCCCAAATTAAATG
TGAGCAGTCTTATGGAACCAACTCCAGTGACGAATCCGGATCGTT
CTCGGAAGCAGACAGTGAGTCGTGTCCTGTGCAGGACAGGGGCC
AGGAGGTAAAACTTCCTTTTCCTGTAGATCAAATCACAGATCTTCC
AAGGAACGATTTCCAGATGATGATTAAAATGCACAAGCTAACCTCA
GAACAGTTAGAGTTTATTCATGATGTCCGACGGCGCAGCAAGAACC
GCATCGCGGCCCAGCGCTGCCGCAAAAGGAAACTGGACTGTATTC
AGAATTTAGAATGTGAAATCCGCAAATTGGTGTGTGAGAAAGAGA

	AACTGTTGTCAGAGAGGAATCAACTGAAAGCATGCATGGGGGAA CTGTTGGACAACTTCTCCTGCCTTTCCCAGGAAGTTTGCCGAGA CATCCAGAGCCCCGAGCAGATCCAGGCCCTGCATCGGTATTGCC CTGTCCTCAGACCCATGGACTTGCCCACGGCCTCCAGTATTAACC CTGCGCCCTTGGGTGCTGAGCAGAACATTGCGGCCTCCCAATGC GCAGTGGGGGAAAACGTGCCCTGCTGCTTGGAGCCAGGCGCGG CTCCCCCCCGGACCCCCCTGGGCACCCAGCAACACCTCCGAGAAT TGTACCTCTGGGAGGAGACTAGAAGGCACTGACCCGGGAACCTT CTCAGAGAGAGGACCTCCTCTTGAACCCAGGAGCCAAACAGTGA CCGTGGACTTCTGCCAGGAAATGACTGATAAGTGTACAACTGAC GAACAGCCCAGGAAAGATTATACCTAG
miR-449b-5p	AGGCAGUGUAUUGUUAGCUGGC
mimic	CAGCUAACAAUACACUGCCUUU

Note: The mutants of binding sites are marked red. WT: wide-type; MT: mutant.

Table S3: Antibodies used for IB, IP, ChIP, RIP and IF assays

Antibodies	Source	Antibody dilution	Identifier
Western blotting			
Rabbit anti-GFPT1	Abcam	1:1000	Cat#ab125069
Mouse anti-O-GlcNAc	Abcam	1:1000	Cat#ab2739
Rabbit anti- BACH2	Abcam	1:2000	Cat#ab226394
Rabbit anti- OGT	Abcam	1:1000	Cat#ab96718
Rabbit anti-CD9	Abcam	1:1000	Cat# ab236630
Mouse anti-TSG101	Abcam	1:1000	Cat# ab83
Rabbit anti-HA	Cell Signaling Technology	1:1000	Cat#3724
Rabbit anti- DYKDDDDK	Cell Signaling Technology	1:1000	Cat#14793
Rabbit anti-Calnexin	Cell Signaling Technology	1:1000	Cat# 2679
SLC7A11	Proteintech	1:1000	26864-1-AP
GPX4	Proteintech	1:2000	67763-1-Ig
Mouse anti-β-actin	Proteintech	1:5000	Cat# 66009-1-Ig
Rabbit anti-PCNA	Proteintech	1:5000	Cat# 10205-2-AP
Mouse anti-GAPDH	Proteintech	1:5000	Cat# 60004-1-Ig
Rabbit anti-KPNA1	Proteintech	1:1000	Cat# 18137-1-AP
Rabbit anti-UMOD	R&D Systems	1:1000	Cat# MAB5175
IP			
Mouse anti-DYKDDDDK-Tag	Abmart	1:100	Cat# M20008
Mouse anti-HA-Tag	Abmart	1:100	Cat# M20003
Rabbit anti-OGT	Abcam	1:100	Cat# ab96718
Rabbit anti-BACH2	Abcam	1:100	Cat# ab226394
sWGA-conjugated agarose beads	Vector Laboratories	1:10	Cat# AL-1023S
Protein A/G magnetic beads	MCE	-	Cat# HY-K0202
ChIP			
Rabbit anti-HA	Cell Signaling Technology	1:50	Cat#3724
RIP			
Rabbit anti-AGO2	Abcam	1:50	Cat#ab186733
Rabbit anti-GFP	Abcam	1:50	Cat#ab290
IF			
Rabbit anti- OGT	Abcam	1:1000	Cat# ab96718
SLC7A11	Proteintech	1:500	26864-1-AP
Mouse anti-HA-Tag	Abmart	1:1000	Cat# M20003
DAPI	Cell Signaling Technology	1:100	Cat# 4083
Goat anti-Rabbit IgG (Alexa Fluor® 488 Conjugate)	Cell Signaling Technology	1:500	Cat# 4412
Goat Anti-Mouse IgG (Alexa Fluor® 555 Conjugate)	Cell Signaling Technology	1:500	Cat# 4409
Goat Anti- Rabbit IgG (Alexa Fluor® 647 Conjugate)	Cell Signaling Technology	1:500	Cat# 4414

Table S4: Chemicals, commercial assays and experimental models used in the study

Resource	Source	Identifier
Chemicals		
2× Taq PCR Green Mix	Takara	RR820A
RNAiso Plus	Takara	9108
PNGaseF (Glycerol-free), Recombinant	New england biolabs	P0709S
PUGNAc	Sigma–Aldrich	A7229
OSMI-1	Sigma–Aldrich	SML1621
Ferrostatin-1	Sigma–Aldrich	SML0583
MG132	Sigma–Aldrich	M7449
CHX	Sigma–Aldrich	5087390001
D-2-Deoxyglucose	Sigma–Aldrich	D8375
Antimycin A	Sigma–Aldrich	A8674
Lipofectamine 2000	Invitrogen	11668019
Lipofectamine 3000	Invitrogen	L3000015
GW4869	MCE	HY-19363
Critical commercial assays		
BCA protein assay Kit	Thermo Fisher Scientific	23227
Nuclear and Cytoplasmic Protein Extraction Kit	Thermo Fisher Scientific	78833
DAB kit	Thermo Fisher Scientific	34002
Cell lysis buffer for Western and IP	Beyotime	P0013
RIPA	Beyotime	P0013B
PMSF	Beyotime	ST506
4% Paraformaldehyde	Beyotime	P0099
Penicillin-Streptomycin	Beyotime	C0223
Lipid Peroxidation MDA Assay Kit	Beyotime	S0131S
Cell Counting Kit-8	Dojindo	CK04
Dual-Luciferase® Reporter Assay System	Promega	E1910
PVDF membranes	Millipore	ISEQ00010
Magna RIP™ RNA-Binding Protein Immunoprecipitation Kit	Millipore	17-700
PrimeScript® RT reagent Kit	Takara	RR047A
Mir-X miRNA First-Strand Synthesis Kit	Takara	638313
Protease Inhibitor Cocktail	Bimake	B14001
Dulbecco's modified Eagle's medium	Gibco	C11995500BT
DMEM/F12	Gibco	11320033
Foetal bovine serum	BioInd	04-001-1A
Bovine serum albumin	Sigma–Aldrich	V900933
PKH67	Sigma–Aldrich	MINI67
PKH26	Sigma–Aldrich	MINI26
EDTA	Solarbio	E1170
Reduced Glutathione (GSH) Colorimetric Assay Kit	Elabscience	E-BC-K030-M
Ferrous Iron Colorimetric Assay Kit	Elabscience	E-BC-K773-M

Cell lines		
HK-2	Cell Bank of the Chinese Academy of Sciences	SCSP-511
293T	Cell Bank of the Chinese Academy of Sciences	GNHu17
Experimental models		
C57BL/6-Gfat1$^{+/-}$ mice	Shanghai	SHANGHAI MODEL ORGANISMS
C57BL/6	Beijing	Beijing Speifu Biotechnology Co., Ltd